

# STOCHASTIC RESOLUTION ANALYSIS OF CO-PRIME ARRAYS IN RADAR

*Radmila Pribić\**    *Mario Coutino†*    *Geert Leus†*

\*Sensors Advanced Developments, Thales Nederland, Delft, The Netherlands

†Delft University of Technology, Delft, The Netherlands

## ABSTRACT

Resolution from co-prime arrays and from a full ULA of the size equal to the virtual size of co-prime arrays is investigated. We take into account not only the resulting beam width but also the fact that fewer measurements are acquired by co-prime arrays. This fact is relevant in compressive acquisition typical for compressive sensing. Our stochastic approach to resolution uses information distances computed from the geometrical structure of data models that is characterized by the Fisher information. The probability of resolution is assessed from a likelihood ratio test by using information distances. Based on this information-geometry approach, we compare stochastic resolution from active co-prime arrays and from the full-size ULA. This novel stochastic resolution analysis is applied in a one-dimensional angle processing. Results demonstrate the suitability in radar-resolution analysis.

**Index Terms**— resolution, information geometry, co-prime arrays, compressive sensing, radar

## 1. INTRODUCTION

Resolution is primarily given by the minimum distance between two objects that still can be resolved (e.g.[1]). For the performance guarantees, a complete resolution description needs also the probability of resolution at a given separation and signal-to-noise ratio (SNR).

For the stochastic completeness, we keep exploring information geometry (IG) and compressive sensing (CS) in radar ([2]). IG is stochastic signal processing whose inferences are structures in differential geometry (e.g. [3-4]). The intrinsic geometrical structure of measurement models is characterized by the Fisher information metric (FIM). Accordingly, potential resolution of sensors is based on information distances on such statistical manifolds. The FIM is typically applied in the accuracy analysis to obtain the Cramer-Rao bound (CRB) of the mean squared error (MSE). In the IG-based resolution analysis, the FIM is also a fundament for computing bounds in resolution that are called information resolution.

The resolution ability is primarily given by the sensing bandwidth. In angle processing, it is determined by the wavelength and the antenna aperture size: either actual as in a full uniform array or virtual as in the case of co-prime arrays. Our analysis includes SNR and processing gain (PG) as being critical with the acquisition of fewer samples what is typical for CS. For the completeness of the stochastic resolution, we also assess the probability of

resolution from a generalized likelihood ratio (GLR) test by using information distances.

As we focus on the system level of CS, we also check how the resolution limits are related to the high-resolution performance of sparse-signal processing (SSP). SSP is nowadays a major part of CS. CS is also optimized to information in measurements. The optimization is based on the two conditions: sparsity of processing results and the sensing incoherence (e.g. [5]). In radar, SSP can be seen as a refinement of existing processing (e.g. [6-7]). SSP is crucial in the back end of a sensor with CS, while its front end facilitates compressive acquisition of measurements. When fewer measurements are enabled already before reception as in the case of co-prime arrays, the compressive acquisition is usually called sparse sensing (e.g. [8]). Compressive acquisition makes also overall PG, certainly PG from SSP, additionally important. Optimal PG from SSP can be achieved if spatial measurements (needed for angles) are combined with temporal measurements (needed for range and Doppler).

Both IG and CS can improve radar performance (and perhaps also lower the costs) because the demands of data acquisition and signal processing can be optimized to the information content in radar measurements rather than to the sensing bandwidth only. Our resolution analysis with IG and CS is novel, and also understood in practical cases.

In this paper, we focus on resolution potential from fewer measurements acquired by active co-prime linear arrays (LAs). Moreover, since we keep exploring CS at the system level, we also investigate the back-end by checking how far the SSP resolution is from the resolution limits.

### 1.1. Related Work

Information resolution has been studied (e.g. [2], [4], [9] and [10]) but not related to the resolution limits from co-prime arrays or compressive acquisition as typical for CS. Stochastic resolution limits have also been studied (e.g. [11] and [12]) but not by using IG.

### 1.2. Outline and Main Contributions

In Section 2, co-prime LAs are presented in active radar (as also indicated in [8]). SSP with measurements from co-prime LAs is also given (as in [10] with main contributions of suitability of co-prime LAs to SSP with optimal PG).

In Section 3, our stochastic resolution analysis is introduced with main contributions of including the probability of resolution via a GLR test with information distances. In Section 4, numerical results from SSP and the stochastic resolution analysis are compared. In the end, conclusions are drawn and future work indicated.

## 2. CO-PRIME ARRAYS IN ACTIVE CS RADAR

In standard CS, compressive acquisition applies after reception as analog-to-information conversion (AIC, e.g. [5]). In radar, such AIC causes drawbacks such as: analog computations, SNR loss, stochastically changed radar data, etc. Therefore, we investigate compressive acquisition before reception, i.e. sparse sensing, and moreover, try exploring the existing means in a radar system design: waveforms and antenna arrays (AA) for temporal and spatial acquisition, respectively (e.g. [10]).

In this work, we keep exploring AAs for spatial sparse sensing with co-prime LAs, and focus on the angular resolution limits. Moreover, while focusing on the system level, we also assess the SSP performance in the back-end.

### 2.1. Co-prime linear arrays

Co-prime arrays are defined by a pair of uniform LAs (ULAs) formed by  $M$  and  $L$  elements and with spacing of  $Ld$  and  $Md$ , respectively, where  $M$  and  $L$  are co-prime integers (i.e. with no common divider) and  $d$  is usually equal to the half-wavelength [8]. An  $(M, L)$  co-prime array is shown in Fig. 1, for  $M = 6$  and  $L = 5$ .



Fig. 1. Positioning of elements (blue) of an  $(M, L)$  co-prime array with  $M=6$  and  $L=5$ . From  $30d$  (grey) it would repeat.

Due to the co-prime sampling, there are  $ML$  distinct phase shifts, i.e.  $ML$  distinct (virtual) positions which imply a high-resolution potential with a reduced number of samples. Namely, a resolution of the order  $1/ML$  can be achieved by  $(M, L)$  co-prime arrays from  $(M, L)$  DFT filter banks (Fig.2 in [8]). Each output is defined as:  $H_m(e^{j\omega}) = H(e^{j(\omega-2\pi m/ML)L})$  and  $G_l(e^{j\omega}) = G(e^{j(\omega-2\pi l/ML)M})$ , for  $0 \leq m \leq M-1$ ,  $0 \leq l \leq L-1$ , and  $\omega = \pi \sin\theta$ . The product  $F_{lm}(e^{j\omega})$  of the  $m^{\text{th}}$  and  $l^{\text{th}}$  outputs:

$$F_{lm}(e^{j\omega}) = G(e^{j(\omega-2\pi l/ML)M})H(e^{j(\omega-2\pi m/ML)L}) \quad (1)$$

is characterized by a unique pass-band with width  $2\pi/ML$ . Thus, there is only one overlapping beam among  $M$  beams of  $G_l(e^{j\omega})$  and  $L$  beams of  $H_m(e^{j\omega})$ , as indicated in Fig. 2. Moreover, the distinct  $ML$  overlapping beams are equivalent to the beams from a ULA with  $ML$  elements.

The processing of co-prime arrays is usually based on covariance estimation (e.g. [8]) which is less convenient for radar than the processing in [10] summarized here.

### 2.2. SSP with co-prime AA measurements

Raw radar measurements  $\mathbf{y}$  (e.g. [13]) can be modeled as:

$$\mathbf{y} = \mathbf{A}\mathbf{x} + \mathbf{z}, \quad (2)$$

by a sensing matrix  $\mathbf{A} \in \mathbb{C}^{K \times N}$ , a sparse profile  $\mathbf{x} \in \mathbb{C}^N$ , signals  $\mathbf{A}\mathbf{x}$  and a (complex Gaussian) receiver-noise vector  $\mathbf{z}$  of i.i.d. elements with zero mean and equal variances  $\gamma$ ,  $\mathbf{z} \sim \mathcal{CN}(\mathbf{0}, \gamma \mathbf{I}_K)$ . The usual SSP, e.g. LASSO, applies as:

$$\mathbf{x}_{\text{SSP}} = \arg \min_{\mathbf{x}} \|\mathbf{y} - \mathbf{A}\mathbf{x}\|^2 + \eta \|\mathbf{x}\|_1 \quad (3)$$

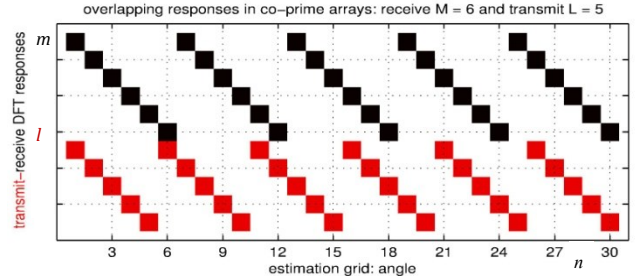


Fig. 2. Unique pairs of  $L$  transmit and  $M$  receive responses from co-prime LAs (with  $M=6$  and  $L=5$ , Fig. 1) over  $ML$  angle cells (as in [8]). Each cell is uniquely represented by a pair  $(H_m, G_l)$ , as given in (1) and utilized in (4).

with the  $l_1$ -norm  $\|\mathbf{x}\|_1$  promoting sparsity, the  $l_2$ -norm  $\|\mathbf{y} - \mathbf{A}\mathbf{x}\|$  minimizing the errors, and a regularization parameter  $\eta$  that balances between the two tasks. In radar, the parameter  $\eta$  is closely related to the detection threshold (e.g. [6-7]). An underdetermined system can be solved,  $K < N$ , because of the sparsity, i.e. only  $S$  nonzeros in  $\mathbf{x}$ ,  $S < K < N$ , and incoherence of  $\mathbf{A}$  (e.g. [5]). The mutual coherence  $\kappa(\mathbf{A})$  is an incoherence measure,  $\kappa(\mathbf{A}) = \max_{i,j,i \neq j} |\mathbf{a}_i^H \mathbf{a}_j|$  where  $\mathbf{a}_n$  is an  $n^{\text{th}}$  column of  $\mathbf{A}$ ,  $\|\mathbf{a}_n\| = 1$ ,  $n = 1, \dots, N$ .

In radar processing, a sensing matrix  $\mathbf{A}$  is intrinsically deterministic and its incoherence is also intrinsically strong because of the physics of radar sensing. Typical radar-sensing data models employ shifts of a transmitted signal in time, in frequency and in phase for processing of range, Doppler and angles, respectively (e.g. [13]). For example, in ULA processing,  $\mathbf{A}$  from (2) is an IFFT matrix, i.e.  $\kappa(\mathbf{A}) = 0$ , without up-sampling of the estimation grid.

The SSP from (3) uses complex-valued measurements directly which are preferred in radar because of processing gain (PG, e.g. [13]). The covariance-based processing leads to power-based SSP, and moreover, it can hardly treat all radar parameters: range, Doppler and angles, at once as desired for optimal PG in CS radar [10].

Therefore, we prefer exploring transmit-receive co-prime arrays as suitable for active radar [10]. As indicated in [8], with  $M$  transmit and  $L$  receive elements, an outcome  $C_{mn}(t)$  of an  $m^{\text{th}}$  receive filter (known for all  $ML$  angles, [8] and Fig. 2),  $0 \leq m \leq M-1$ , at time  $t$  and angle  $\theta_n$ ,  $\omega_n = \pi \sin\theta_n$ ,  $0 \leq n \leq N-1$ ,  $N = ML$ , is modeled [10] as:

$$C_{m,n_{ml}}(t) = \sum_{j=0}^{L-1} \alpha_{n_{mj}}(t) (H_{m,n_{mj}} G_{l,n_{mj}}) + Z_m(t) \quad (4)$$

where  $\alpha_n(t)$  is an echo at  $t$  from  $\omega_n$ , a pair  $(m, l)$  is unique for  $\omega_{n_{ml}}$ ,  $H_{mn}$  and  $G_{ln}$  are responses of the  $m^{\text{th}}$  receive, and an  $l^{\text{th}}$  transmit filter (interpreted over all  $ML$  angles, as in Fig. 2), respectively, and  $Z_m(t)$  is the DFT of the noise. The PG from  $H_{mn}$  and  $G_{ln}$  equals  $M$  and  $L$ , respectively.

The received data  $C_{mn}(t)$  contain already the products  $H_{mn}G_{ln}$  and moreover, the temporal part  $\alpha_n(t)$  remains complex-valued. Finally, we create an  $N \times 1$  data vector  $\mathbf{c}(t)$  with elements  $c_n(t) = \sum_{m=1}^M C_{mn}(t)$ , and build a model with a vector  $\mathbf{y}(t)$  coming from the inverse DFT of the  $M$  received data sorted in  $\mathbf{c}(t)$ , as:

$$\mathbf{y}(t) = \mathbf{F}\mathbf{c}(t) = \mathbf{F}\mathbf{x}(t) + \mathbf{z}(t), \quad (5)$$

where  $\mathbf{F}$  is an  $ML \times N$  steering matrix whose  $n^{\text{th}}$  column:  $\text{vec}[\mathbf{g}_n \mathbf{h}_n^T]$  at  $\omega_n$ , has  $ML$  distinct (virtual) positions  $i$ ,  $i \in$

$\{0 L M \dots 2ML-(M+L)\}$ . The values  $h_{m,n}$  and  $g_{l,n}$  can be written as:  $h_{m,n} = e^{jml\omega_n}$  and  $g_{l,n} = e^{jlm\omega_n}$ , respectively. Such a steering matrix  $\mathbf{F}$  applies also to an LA of size  $N$ ,  $N = ML$ . The PG from  $\mathbf{F}$  equals  $ML$ ,  $PG = \|\mathbf{f}_n \alpha_n\|^2 / |\alpha_n|^2$ .

Hence, only  $M$  received data are acquired by the AA for an  $N \times 1$  angle profile  $\mathbf{x}(t)$ ,  $M < N$ ,  $N = ML$ , directly with less AA elements and without AIC. The data  $\mathbf{y}(t)$  from (5) can include Doppler and range by modeling  $\mathbf{x}(t)$  over coherent processing time  $t$ . (Coherence means in radar processing that the phase is preserved which differs from coherence  $\kappa(\mathbf{A})$  in CS). This complex-valued time-space SSP ([10]) gives more PG than the power-based SSP.

### 3. STOCHASTIC RESOLUTION ANALYSIS

Our stochastic resolution analysis is based on information geometry (IG). IG is the study of manifolds in the parameter space of probability distributions, using the tools of differential geometry (e.g. [3-4]). The inner product of two vectors  $\mathbf{x}$  and  $\mathbf{y}$  in a Euclidean space:  $\langle \mathbf{x}, \mathbf{y} \rangle = \mathbf{x}^H \mathbf{y}$  is redefined as:  $\langle \mathbf{x}, \mathbf{y} \rangle = \mathbf{x}^H \mathbf{Q} \mathbf{y}$ , where  $\mathbf{Q}$  is a metric tensor defined by the FIM in IG. The FIM makes the length differ from the length in Euclidean space. The shortest path between two points is called a *geodesic* which is the extension of a straight line to non-Euclidean spaces. For example, on a spherical surface there are no straight lines, so that the geodesic is the shorter great circle arc.

Stochastic resolution analysis is applied to an  $(M, L)$  co-prime array of size  $M+L$  as compared to a full ULA of size  $ML$ . In both arrays, a received signal  $y_i$  at an array-element position  $\mu_i$  (measured in half-wavelength units, and centered for zero mean,  $\sum_i \mu_i = 0$ ) can be modeled as in (5):

$$y_i = \alpha e^{j\mu_i \omega} + z_i = \alpha a_i(\omega) + z_i, \quad (6)$$

where  $\alpha$  is a target echo,  $\omega$  is the angle parameter,  $\omega = \pi \sin \theta$  (as in Section 2),  $a_i(\omega) = e^{j\mu_i \omega}$ , and  $z_i$  is the receiver noise,  $z_i \sim CN(0, \gamma)$ . For fair comparison, the transmit PG is ignored and an input echo  $\alpha_{in}$  is equal and constant (so-called SW0, e.g. [13]). The receive PG is  $M$  in the co-prime array and  $ML$  in the full ULA. The model from (6) applies where  $\alpha$  and  $ML$  positions  $\mu_{in,i}$  differ as:

- ULA:  $\alpha = \alpha_{in}$  and  $\mu_{in,i} \in \{0 \ 1 \ 2 \ \dots \ ML - 1\}$ ; and
- co-prime:  $\alpha = \alpha_{in} / \sqrt{L}$  and virtual positions  $\mu_{in,i}$  from  $\mathbf{F}$  as given in (5),  $\mu_{in,i} \in \{0 \ L \ M \ \dots \ 2ML-(M+L)\}$ .

The positions  $\mu_{in,i}$  are centered:  $\boldsymbol{\mu} = \boldsymbol{\mu}_{in} - \bar{\boldsymbol{\mu}}_{in}$ , so that  $\bar{\boldsymbol{\mu}} = 0$ .

The Fisher information metric  $Q(\omega)$  for the angle parameter  $\omega$  can be written as (e.g. [10] and [14]):

$$Q(\omega) = -E \left[ \frac{\partial^2 \ln p(\mathbf{y}|\omega)}{\partial \omega^2} \right] = 2 \frac{|\alpha|^2}{\gamma} \sum_i \mu_i^2 = 2 \text{SNR} \sum_i \mu_i^2 \quad (7)$$

for a Gaussian pdf  $p(\mathbf{y}|\omega)$  of  $\mathbf{y}$  and unknown  $\omega$  from (6).

In the accuracy analysis, the metric  $Q(\omega)$  is typically applied to the Cramer-Rao bound (CRB) of the mean squared error (MSE) of an unbiased estimator  $\hat{\omega}$  of  $\omega$ , i.e.  $\text{MSE}(\hat{\omega}) \geq \text{CRB}(\omega) = 1/Q(\omega)$  (e.g. [14]).

In addition,  $Q(\omega)$  can be used to compute the Fisher-Rao information distance (FRID) between  $p(\mathbf{y}|\omega)$  and  $p(\mathbf{y}|\omega + \delta\omega)$  on the 1D statistical manifold (e.g. [10]), as:

$$d(\omega, \omega + \delta\omega) = \int_{\omega}^{\omega + \delta\omega} \sqrt{Q(u)} \, du = \delta\omega \sqrt{2 \text{SNR} \sum_i \mu_i^2}. \quad (8)$$

In [10], we compared FRIDs because our goal was to assess changes in information resolution of different LAs. In this study, we derive the information resolution from  $d(\omega, \omega + \delta\omega_0)$  at a separation  $\delta\omega_0$  and an SNR at which two angles can be resolved with a certain probability.

In some early work on IG [15], Rao proposed a test statistic  $w_\omega$ ,  $w_\omega$  from  $N(0,1)$ , for testing a hypothesis  $H_0: \delta\omega = 0$  and its alternative  $H_1: \delta\omega \neq 0$ , given by:

$$w_\omega = \frac{\hat{d}_\omega}{\sqrt{\text{var}[\hat{d}_\omega]}} \xrightarrow{a} \frac{d(\omega, \omega + \delta\omega)}{\sqrt{\text{CRLB}[d(\omega, \omega + \delta\omega)]}} = \frac{\delta\omega}{\sqrt{\text{CRLB}[\delta\omega]}} \quad (9)$$

where a distance estimate  $\hat{d}_\omega$  is (asymptotically) Gaussian-distributed and normalized by its standard deviation. The proposed distance  $d_\omega$  was actually FRID,  $d_\omega = d(\omega, \omega + \delta\omega)$ , as clearly hinted by giving an example in [15]. We also keep using FRID as it is directly related to the basic IG infinitesimal metric  $ds$ ,  $ds^2 = d\boldsymbol{\theta}^T \mathbf{G}(\boldsymbol{\theta}) d\boldsymbol{\theta}$  where  $\boldsymbol{\theta}$  is the parameter vector,  $\boldsymbol{\theta} = [\omega]$  here. FRID is a geodesic computed from the integrals of  $ds$  over possible curves of integration. Finally, most IG (pseudo-)distances reduce to simple functions of FRID.

In the azimuth-only case, the statistic  $w_\omega$  remains the same with  $d(\omega, \omega + \delta\omega)$  or with the Euclidean distance  $\delta\omega$ . In a realistic (radar) case with more parameters, it is not the case any more. For instance, in the azimuth-elevation case,  $\boldsymbol{\theta} = [u \ v]^T$ , the statistic  $w_{u,v}$  would be:

$$w_{u,v} = \frac{\hat{d}_{u,v}}{\text{std}[\hat{d}_{u,v}]} \xrightarrow{a} \frac{\|\boldsymbol{\mu}_x \delta u + \boldsymbol{\mu}_y \delta v\|}{\sqrt{\text{CRLB}[\|\boldsymbol{\mu}_x \delta u + \boldsymbol{\mu}_y \delta v\|]}}$$

where  $u$  and  $v$  indicate azimuth and elevation, respectively, and vectors  $\boldsymbol{\mu}_x$  and  $\boldsymbol{\mu}_y$  contain positions of planar antenna-array elements in  $x$  and  $y$  directions, respectively. The FRID contains weighted ( $\|\boldsymbol{\mu}_x \delta u + \boldsymbol{\mu}_y \delta v\|$ ) rather than direct separations:  $\|\delta\boldsymbol{\theta}\| \equiv \sqrt{\delta u^2 + \delta v^2}$ . In addition, although the parameter space in radar is multidimensional, the FRID remains one-dimensional which simplifies our perception of the resolution results.

The test with  $w_\omega$  from (9) is only concerned with  $H_0$  i.e. rejecting  $H_0$  could only suggest that  $H_1$  might be true, while we prefer assessing  $H_1$  directly. Namely, in the resolution analysis here, we focus on assessing the resolution potential when there are two close targets. Thus, we prefer assessing  $H_1: \delta\omega \neq 0$ . Hence, we study the same hypothesis from (9):  $H_0: \delta\omega = 0$  and  $H_1: \delta\omega \neq 0$ , but with a generalized likelihood ratio (GLR) given by:

$$\text{GLR} = p(\mathbf{y}|\omega, \omega + \delta\omega) / p(\mathbf{y}|\omega) |_{\delta\omega = \delta\omega_{\text{ML}}}, \quad (10)$$

where  $\delta\hat{\omega}_{\text{ML}}$  is the maximum likelihood (ML) estimate of  $\delta\omega$ , and  $p(\mathbf{y}|\omega, \omega + \delta\omega) / p(\mathbf{y}|\omega)$  is the likelihood ratio (LR) at the true separation  $\delta\omega$  where data  $\mathbf{y}$  as in (2) and (6) contain responses from two point-targets separated by  $\delta\omega$ . Thus, testing the hypothesis from (10):  $H_1: \delta\omega \neq 0$  and  $H_0: \delta\omega = 0$ , is related to  $\mathbf{y} = \alpha \mathbf{a}(\omega) + \alpha \mathbf{a}(\omega + \delta\omega) + \mathbf{z}$  under  $H_1$  and  $\mathbf{y} = 2\alpha \mathbf{a}(\omega) + \mathbf{z}$  under  $H_0$ .

Next we investigate how  $\ln \text{GLR}$  statistic is related to  $d_\omega$  and  $w_\omega$  from (8). The asymptotic  $\ln \text{GLR}$  is  $\chi^2$ -distributed with one degree of freedom ([16] and [12]): centrally (under  $H_0$ ) and non-centrally (under  $H_1$ ) with the parameter  $\varepsilon$  given by:  $\varepsilon = \delta\omega^2 Q(\omega)$ ,  $\ln \text{GLR} \sim \chi_{\varepsilon, 1}^2$ . We can

notice that  $\varepsilon$  is directly related to the FRID  $d_\omega$  as:  $\varepsilon = d_\omega^2$  where  $d_\omega$  is a FRID from (8). Rao's test statistic  $w_\omega$  is related to  $\varepsilon$  only under  $H_0$  as:  $w_\omega \sim N(\sqrt{\varepsilon}, 1)$ ,  $\varepsilon = 0$ .

Finally, we can test ln GLR statistics,  $\ln \text{GLR} \sim \chi_{\varepsilon,1}^2$ , from the non-central  $\chi^2$ -distribution (under  $H_1$ ) with  $\varepsilon$ ,  $\varepsilon = d_\omega^2$ , against an asymptotic-GLRT threshold  $\rho$  at constant probability of false alarms  $P_{fa}$ ,  $\rho = \chi_{0,1}^{2,\text{inv}}(P_{fa})$ . The probability of resolution  $P_{\text{res,IG-GLRT}}$  can be written as:

$$P_{\text{res,IG-GLRT}} = \text{P}\{\ln \text{GLR} > \rho \mid H_1\}. \quad (11)$$

The stochastic FRID-based probability  $P_{\text{res,IG-GLRT}}$  is assessed numerically together with the probability of resolution  $P_{\text{res,SSP}}$  from the SSP solution  $\mathbf{x}_{\text{SSP}}$  in (3) given for two point-targets at positions  $i$  and  $j$ ,  $i \neq j$ , by:  $P_{\text{res,SSP}} = \text{P}\{(x_{\text{SSP},i} \neq 0) \wedge (x_{\text{SSP},j} \neq 0) \mid H_1\}$  where the SSP regularization parameter  $\eta$  in (3) is related to the same false-alarm probability  $P_{fa}$  as:  $\eta = \sqrt{-\gamma \ln P_{fa}}$  (e.g. [6]).

#### 4. NUMERICAL RESULTS

Results on LAs and our stochastic resolution analysis are shown together with the SSP resolution performance.

##### 4.1. Co-prime arrays and SSP

Resolution of an  $(M,L)$  co-prime array ( $M=6$  and  $L=5$  as in Fig. 1) is indicated by a single beam of all the  $ML$  beam responses, in Fig. 3a. The co-prime response is comparable with the response of a ULA with  $ML$  elements (Fig. 3b).

Angle processing from (5) with  $(M,L)$  co-prime array measurements from (4) is shown in Fig. 4. SSP from (3) is performed with `yall1` ([17]) at  $\eta = 3$ . There are  $S$  non-zeros randomly located over the estimation grid,  $S > M+L$ . The true amplitude  $\alpha$  of a nonzero in  $\mathbf{x}$  is constant (so-called SW0 in radar) and given by its SNR,  $\text{SNR} = |\alpha|^2 / \gamma$ ,  $\gamma=1$ .

##### 4.2. Stochastic resolution analysis

Our stochastic resolution analysis (presented in Section 3) is shown in angle processing with two close targets whose

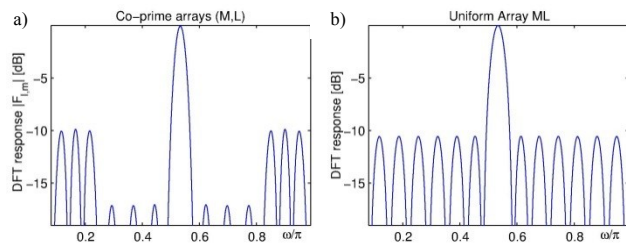


**Fig. 3.** A beam (of all  $ML$  beams) of: a) an  $(M,L)$  co-prime array (Fig. 2) and b) a ULA with  $ML$  elements.

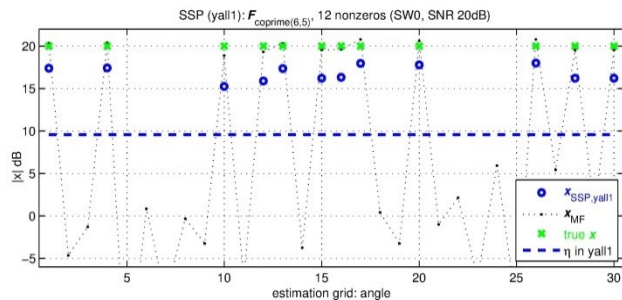


**Fig. 4.** Results of SSP from (5) with  $S$  angles and  $(M,L)$  co-prime LAs,  $S > M+L$ ,  $S=12$ , and  $M=6$  and  $L=5$  as in Fig. 2.

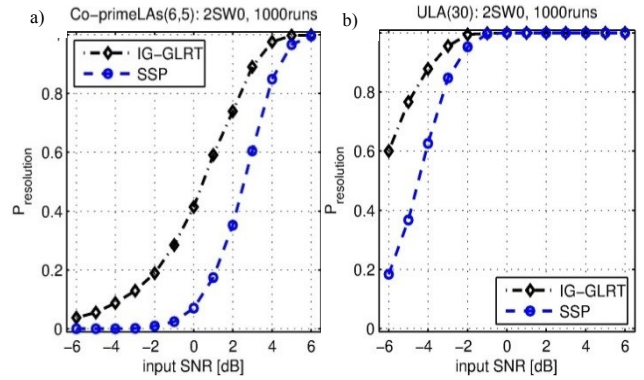


**Fig. 5.** Resolution bounds via IG-based GLR test (IG-GLRT) and SSP resolution from: a) co-prime LAs (Fig. 2) and from b) a full ULA. Two targets are separated by  $\delta\omega/\pi$  of  $2/ML$ .

measurements are acquired from an  $(M,L)$  co-prime array and from the full ULA of size  $ML$ . Two targets are separated by  $\delta\omega/\pi$  of  $2/ML$ , i.e. a DFT bin (in both arrays shown in Fig.3) at different input SNRs. The amplitude  $\alpha_{in}$  is constant,  $|\alpha_{in}|^2 = \gamma \text{SNR}$ ,  $\gamma=1$ , and  $\eta = 3$  in SSP from (3).

The probabilities  $P_{\text{res,IG-GLRT}}$  and  $P_{\text{res,SSP}}$  are assessed numerically from a sufficient number of noise runs. The full receive ULA gives higher  $P_{\text{res,IG-GLRT}}$  at lower SNR mostly because of higher PG due to stronger  $|\alpha|^2$  by 5 (7 dB) as obvious in Fig. 5. Per a single  $\omega$ ,  $Q(\omega)$  differs in  $|\alpha|^2 \sum_i \mu_i^2$  (also in CRLB) by 2.6 (4.1 dB) and 0.52 (-2.9dB) in  $\sum_i \mu_i^2$ . The whole co-prime PG of  $ML$  would make  $P_{\text{res,IG-GLRT}}$  comparable. Now it is the case at higher SNR.

The SSP resolution given by  $P_{\text{res,SSP}}$  is close to the resolution bounds  $P_{\text{res,IG-GLRT}}$  in both cases: 2 dB SNR far at the probability of resolution equal to 0.5, or less at higher values of the probability of resolution.

#### 5. CONCLUSIONS

A stochastic resolution analysis is presented that enables computing resolution bounds based on an information-geometry approach. The bounds are expressed by a probability of resolution at a given separation and SNR.

The resolution bounds are crucial when using co-prime arrays or other spatial sparse sensing in the front-end. In the back-end of a sensor with CS, the resolution bounds are also relevant for evaluating the SSP high-resolution performance. Thus, we consider not only the beam width that depends on the array configuration, but also the effects of fewer measurements that are acquired by sparse sensing. The PG effects can be seen in our resolution bounds as they are based on information distances from IG.

This IG approach to resolution analysis enables us to conclude that active co-prime LAs with  $(M+L)$  elements perform as the full ULA with  $ML$  elements only at higher SNR. Moreover, we can also conclude that the stochastic resolution analysis is appropriate in radar because of the completeness of the impacts that are crucial for the performance guarantees: the AA configuration as well as input SNR, separation and a probability of resolution.

In future work, this stochastic resolution analysis will be applied to other sparse sensing in the front-end, and to all radar parameters: both angles and range and Doppler.

## REFERENCES

- [1] A. J. den Dekker and A. van den Bos, "Resolution: a survey", *J. of the Opt. Soc. of America A*, 14/3, 1997.
- [2] E. de Jong and R. Pribić, "Sparse signal processing on estimation grid with constant information distance applied in radar", *EURASIP Journal on Advances in SP*, 2014:78.
- [3] S. Amari, "Information geometry of statistical inference - an overview", *IEEE IT Workshop*, 2002.
- [4] Y. Cheng, X. Wang, T. Caelli, X. Li and B. Moran, "On information resolution of radar systems", *IEEE Trans on AES* 48/4, 2012.
- [5] D. Donoho, "Compressed sensing," *IEEE Trans. on IT* 52/4, 2005.
- [6] R. Pribić and I. Kyriakides, "Design of Sparse-signal processing in Radar Systems," *IEEE ICASSP* 2014.
- [7] H.L. Yap and R. Pribić, "False Alarms in Multi-Target Detection within a Sparsity Framework", *SEE Radar* 2014.
- [8] P.P. Vaidynathan and P. Pal, "Sparse Sensing With Co-Prime Samplers and Arrays", *IEEE Trans. SP* 59/2, 2011.
- [9] Y. Cheng, X. Wang, and B. Moran, "Angular Information Resolution Limit of Sensor Arrays", *IEEE SAM* 2014.
- [10] R. Pribić, "Angular Information Resolution from Co-prime Arrays in Radar", *EuSiPCo* 2015.
- [11] S. T. Smith, "Statistical resolution limits and the complexified CR bounds", *IEEE Trans. on SP* 53/5, 2005.
- [12] Zhi Liu and A. Nehorai, "Statistical angular resolution limit for point sources", *IEEE Trans. on SP* 55/11, 2007.
- [13] C. E. Cook and M. Bernfeld. *Radar signals; an introduction to theory and application*. Acad.Press, 1967.
- [14] H. L. Van Trees. *Optimum Array Processing*. Wiley, 2002.
- [15] C. R. Rao. Information and the accuracy attainable in the estimation of statistical parameters. *Bull. Calcutta Math.Soc.* 37, pp. 81-89, 1945.
- [16] S.M Kay. *Fundamentals of Statistical Signal Processing Vol. II: Detection Theory*. Prentice Hall, 1998.
- [17] yall1: your algorithms for L1, <http://yall1.blogs.rice.edu/>.